

The antiproliferative, antimigratory and anticlonogenic effects of *Croton membranaceus* Müll. Arg. (Euphorbiaceae) hydroethanolic root extract in human 22Rv1 castration-resistant prostate cancer cells

Kofi O. YEBOAH¹, Miracle EMOSIVBE¹, Emmanuel A. NTIM², George H. SAM³, George AINOOSON^{1*}

¹ Department of Pharmacology, Kwame Nkrumah University of Science and Technology, Kumasi, Ghana

² Department of Physiology, Kwame Nkrumah University of Science and Technology, Kumasi, Ghana

³ Department of Herbal Medicine, Kwame Nkrumah University of Science and Technology, Kumasi, Ghana

ABSTRACT

This study employed the 22Rv1 *in vitro* model of CRPC to investigate the anticancer effect of the hydroethanolic root extract of *Croton membranaceus* (CMERE). The effects of CMERE on proliferation, migration and colony forming ability of 22Rv1 cells were studied. Isobologram analysis of combined effect of CMERE and enzalutamide, an androgen receptor blocker, on 22Rv1 proliferation, was also investigated. Lastly, selective cytotoxicity of CMERE was investigated using 22Rv1, BPH1 and THP-1 cells. We could show that CMERE inhibited testosterone-dependent and independent 22Rv1 cell proliferation. Moreover, drug combination studies showed that CMERE and enzalutamide may inhibit 22Rv1 cell proliferation via different mechanisms. Additionally, CMERE at all doses significantly inhibited the migration and colony formation of 22Rv1. Lastly, CMERE was selectively toxic to 22Rv1 and BPH1 cells but not to the non-prostate derived cell line THP-1 monocyte-like cells. Thus, CMERE possesses anticancer activity against 22Rv1 CRPC model.

Keywords: 22Rv1, castration-resistant prostate cancer, *Croton membranaceus*, isobologram, selective cytotoxicity

*Corresponding author: E-mail: gkainooson@knust.edu.gh

ORCID:

Kofi O. YEBOAH: 0000-0001-7080-0730

Miracle EMOSIVBE: 0000-0002-3905-4992

Emmanuel A. NTIM: 0000-0002-8003-1127

George H. SAM: 0000-0003-1982-095X

George AINOOSON: 0000-0003-1231-785X

(Received 04 May 2022, Accepted 06 Feb 2023)

INTRODUCTION

Prostate cancer (PCa) is a biologically and clinically heterogeneous malignant condition that originates from the prostate, a small gland below the bladder and anterior to the rectum ¹. It is the second most diagnosed cancer in men globally, with an alarming 1.2 million new cases and 350,000 PCa-related deaths recorded annually ². PCa thus affects millions, chiefly in regions of high human development index ². Nonetheless, low-income nations such as countries in sub-Saharan Africa, Central Asia and South Asia, have the highest rates of annual increase in PCa incidence and deaths despite the lowest documented incidence of the disease, as the disease is believed to be underestimated due to lack of screening, poor access to healthcare and environmental factors ³⁻⁵. This illustrates the nature of PCa disease burden on global healthcare, highlighting the need to understand the disease and design effective treatment modalities.

Given the above, the androgen receptor has been identified as the most important molecular driver of prostate cancer progression ^{6,7}. Thus, inhibiting androgen receptor using androgen deprivation therapy is the mainstay of advanced prostate cancer therapy ^{8,9}. Despite initial positive response, nearly all patients fail to respond to androgen ablation following 2–3 years of ADT, and progress to a stage of the disease known as castration-resistant prostate cancer ⁷. Castration-resistant prostate cancer remains incurable as the newer agents such as enzalutamide, flutamide, apalutamide and darolutamide are less effective ¹⁰. Furthermore, apalutamide and darolutamide are significantly toxic and do not provide a lasting solution despite initial improvement in metastasis-free survival ^{11,12}. For this reason, the need for newer, highly effective and less toxic therapies in the treatment of castration-resistant prostate cancer is clearly highlighted.

Accordingly, plants and their products have proven beneficial for centuries as important sources of drug leads despite the increasing popularity of combinatorial chemistry ¹³. In fact, it is estimated that 25.1% of approved anti-cancer drugs originated from natural products and their derivatives ¹⁴. These products of natural origin may produce cost-effective promising results and fewer untoward effects ¹⁵. One such important plant source is *Croton membranaceus* Müll. Arg. (Euphorbiaceae) which has been safely used as a root decoction in the management of benign prostatic hyperplasia (BPH) and other prostate diseases in various Ghanaian communities ¹⁶. In addition, the cytotoxic effect of the methanolic extract has been demonstrated in human MCF-7 breast carcinoma, DLD-1 colon carcinoma, and PC3 prostate carcinoma cells ¹⁷. However, little is known about the effect of the plant on other aspects of cancer development such as cancer cell migration and metastasis. To the best of the

authors' knowledge, no study has reported on the effect of the plant on CRPC (Castration-resistant prostate cancer). This study therefore sought to investigate the effect of the hydroethanolic root extract of *Croton membranaceus* on castration-resistant prostate cancer.

METHODOLOGY

Plant collection and preparation of hydroethanolic root extract

The roots of *Croton membranaceus* Müll. Arg., locally known as bokum by the Krobos of Ghana, were collected from Kwahu-Asakraka in the Eastern Region of Ghana on the 3rd of January, 2021 and were authenticated by Dr. George H. Sam of the Department of Herbal Medicine, KNUST. A voucher specimen (KNUST/HM1/2021/RO05) was deposited at the Herbarium of the Department of Pharmacognosy, KNUST. Subsequently, the fresh roots of *C. membranaceus* were washed thoroughly, dried in shade and pulverized into a coarse powder. Thereafter, *C. membranaceus* roots were extracted as previously described by Sarkodie *et al.*¹⁸ and Asare *et al.*¹⁶, with slight modifications. Briefly, the hydroethanolic root extract (CMERE) was prepared by dissolving 1 kg of root into 4 L of 70% v/v ethanol. The roots were cold macerated in the solvent for 96 hours after which root materials were removed by decantation and the residues were further dissolved in 2.5 L of 70% ethanol for an additional 72 hours. Subsequently, the supernatant was decanted and filtered using a Whatman No.1 filter paper. The hydroethanolic root extract was concentrated in a rotary evaporator (Buchi Labortechnik Rotavap R-210) at 50°C and further dried in an oven (Gallenkamp OMT Oven, SANYO, Japan) at 50°C. The resulting soft mass was then placed in a desiccator to remove the residual moisture. Afterwards, the extract was stored at 4°C until further use. Percentage yield of 3.8%. was obtained for the hydroethanolic root extract.

Gas chromatography-mass spectrometry analysis of extract

Gas chromatography-mass spectrometry (GC-MS) fingerprinting was performed to identify the possible presence of compounds that may be responsible for the biological effects of the extract. Thus, GC-MS analyses of the hydroethanolic root extract was carried out using a PerkinElmer GC Clarus 580 Gas Chromatograph that is interfaced to a Mass Spectrometer PerkinElmer (Clarus SQ 8 S) and equipped with Elite-5MS (5% diphenyl/95% dimethyl poly siloxane) fused to a capillary column (30 × 0.25 µm ID × 0.25 µm DF). The temperature of the oven was serially set from 80°C with stepwise increments of 10°C/min to 250°C, then 5°C/min to 280°C and holding for 15 mins at 280°C. For GC-MS detection, an electron ionization system was operated in electron impact mode

with ionization energy of 70 eV. As a carrier gas, high purity helium gas was used and programmed at a constant flow rate of 1 mL/min, with an injection volume of 1µL. The temperature of the injector and the ion-source were kept at 250°C and 150 °C, respectively. Subsequently, the mass spectrum of the extract was generated at 70 eV with a scan interval of 0.1 s and fragments from 45 to 450Da were analyzed. The solvent delay and the total GC/MS running time were 0 to 2 mins, and 38 mins, respectively. The mass-detector and the software employed to handle mass spectra and chromatogram used in this analysis were Turbo-Mass and Turbo-Mass ver-6.1.0, respectively. Interpretation of the mass-spectrum GC-MS was conducted using the database of National Institute of Standard and Technology (NIST), which contains over 62,000 patterns ¹⁹.

Cell culture

Human prostate carcinoma cell line 22Rv1 and benign neoplastic cell line (BPH1) were obtained as a gift from the Steroid Hormone Lab of Prof. Dr. Andrew Cato of the Institute of Biological and Chemical Systems (IBCS), Karlsruhe Institute of Technology (KIT), Germany, and routinely cultured in Roswell Park Memorial Institute (RPMI) 1640 medium supplemented with 10% heat-inactivated fetal bovine serum (FBS) plus 1 mM sodium pyruvate, 100 units/mL penicillin and 100 mg/L streptomycin (Sigma, Germany), hereto referred to as complete growth medium. THP-1 monocyte-like cells acquired as a kind donation from Mutocheluh Lab (KNUST), were routinely cultured in complete growth medium supplemented with 2-mercaptoethanol. All cells were grown in sterile T-Flasks (Greiner Bio-One, Germany) of different kinds depending on the experimental conditions. At 80 - 90% confluence, culture media were removed, and adhered cells were washed once with pre-warmed PBS 1X to remove remnant media. The washed cells were then incubated with trypsin/EDTA in an incubator for approximately 5 minutes at 37 °C. Afterwards, the added trypsin was inactivated by the addition of fresh medium containing 10% FBS, and the cell suspension was transferred into sterile Falcon tubes and subsequently spined down at 500 rpm for 5 minutes at room temperature to pellet the cells. THP-1 suspension cells, were not trypsinized but spined directly to pellet the cells. Subsequently, the supernatants were pipetted off and the cells re-suspended in fresh complete medium. Afterwards, cells were either incubated in the appropriate T-flasks or counted and seeded into cell culture plates, depending on the type of assay to be carried out. All cell cultures were maintained at 37°C, 5% of CO₂ and 95% of humidity in an incubator (Herasafe KS Class II) ²⁰.

Cytotoxic effects of *Croton membranaceus* extract and IC₅₀ determination

Briefly, cells were seeded into tissue culture-treated 96-well plates at a seeding density of 5×10^3 cells/well. The cells were allowed to attach overnight and normal growth medium was replaced with treatment medium containing various concentrations of the hydroethanolic root extract (1, 3, 5, 10, 30, 50 and 100 mg/ml). The experiment was repeated three times. The cells were incubated for 72 hours, after which 20 μ L of 3-(4,5-dimethylthiazol-2-yl)-2,5 diphenyl-tetrazolium bromide (MTT) was added to each well and the plate incubated in the dark at 37°C, in 5% CO₂ and 95% humidity for 4 hours. Subsequently, the media with MTT were removed from the wells, and the formed formazan crystals were dissolved by adding 120 μ L of isopropanol to each well. Afterwards, the plate was allowed to stand for 30 minutes following which absorbance was read at 595 nm using microplate reader (iMark™, Bio-Rad). Finally, percentage change in absorbance was calculated as shown below and obtained values were fitted to non-linear regression to obtain the IC₅₀s²¹.

$$\% \text{ Change in Absorbance} = \frac{A_0 - A}{A_0} \times 100 \quad \text{Equation (1)}$$

Where A_0 is the absorbance at the least concentration, and A is the measured absorbance

Antiproliferative effects of CMERE in androgen-dependent and independent 22Rv1 cell proliferation

To investigate the effect of CMERE on testosterone-dependent and independent 22Rv1 cell proliferation, the cell culture medium was charcoal-stripped (hereto referred to as starvation medium) prior to the assay. This was done to deplete the medium off androgens and other steroid hormones that may serve as potential agonists or antagonists on the AR, or may serve as precursors to the production of androgens. Afterwards, 22Rv1 cells were cultured in normal complete growth medium and cells were seeded at a density of 5×10^3 cells/well into tissue culture-treated 96-well plates. Cells were allowed to adhere to the plate overnight after which complete growth medium was replaced with charcoal-stripped medium, and the cells maintained in it for an additional 48 hours. After 48 hours, cells were exposed to either 100 μ L of starvation medium, 10 μ M enzalutamide (positive control) or crude extract (1, 3 and 10 mg/mL) for 72 hours.

For androgen-dependent growth, the starvation medium was supplemented with 10 nM testosterone. After 72 hours, cell proliferation was determined using MTT assay as described previously. Conversely, the starvation medium was not supplemented with testosterone in the assessment of testosterone-independent 22Rv1 cell proliferation²². All experiments were repeated 3 times.

Isobologram analysis of a combination of enzalutamide and CMERE

The individual dose effect curves for the hydroethanolic extract and enzalutamide in inhibiting 22Rv1 cell proliferation, were established in an MTT assay and the respective IC_{50} s determined. The two drugs were combined in various ratios (1:1, 1/2 : 1/2, 1/4 : 1/4, 1/16 : 1/16 and 1/32 : 1/32) of their IC_{50} s and the dose effect curve and median-effect plot for the combination were determined using the software CompuSyn (1.0, Chou-Martin). The potency (D_m)_{1,2} value, the shape (m)_{1,2} value and (r)_{1,2} values for the drug mixture were also obtained using the Compusyn-generated automated median-effect plot (the Chou plot). The r value signifies conformity of the data to the mass-action law. Subsequently, the Chou-Talalay method for drug combination, based on the median-effect equation^{23,24}, was used to determine the combination index (CI) and define additive effect (CI = 1), synergism (CI < 1), and antagonism (CI > 1) in CMERE-enzalutamide combinations. These values were used to generate the fractional inhibition – combination index (Fa-CI) plot, dose-reduction index (Fa-DRI) plot and the classic and normalized isobologram. The following equations are the algorithms for the computerized simulation used to obtain the CI values:

$$\frac{f_a}{f_u} = \left[\frac{D}{D_m} \right]^m,$$

$$\text{Log} \left[\frac{D}{D_m} \right] = m \log(D) - m \log(D_m),$$

$$CI = \sum_{j=1}^n \frac{(D)_j}{(D_x)_j},$$

Where D = Dose, D_m = median effect dose, D_x = dose of each drug that produces X% inhibition, f_a = fraction inhibited, f_u = fraction uninhibited, m = slope

The inhibitory effect of CMERE on migration of 22Rv1 cells

Here, 2×10^5 22Rv1 cells were seeded into 12-well plates. After 24 hours, complete media was replaced with starvation medium and the cells were maintained in it for an additional 48 hours. At 75-90% confluence, monolayers were scratched with a 10 μ L pipette tip. The scratched monolayers were washed twice with phosphate buffered saline (PBS), and starvation medium containing respective treatments as described earlier, was added to respective wells. The experiment was repeated 3 times. Wounds were immediately photographed with a camera attached to a microscope (Nikon, USA) and the cells were afterwards incubated at 37°C, in 5% CO₂ and 95% humidity for 72 hours. Wounds were again photographed at 24, 48 and 72 hours after scratching²⁰. The migrated distances by

the cells across the wounds were determined using ImageJ 1.46r software (NIH, USA) and percentage changes in wound area were calculated as shown below:

$$\% \text{ Change in wound area} = \frac{A_0 - A_t}{A_0} \times 100$$

Where A_0 is the wound area at 0 hour, and A_t is the wound area at time, t

Effect of CMERE on colony formation of 22Rv1 cells

Cells were seeded into tissue culture-treated 6-well plates at a seeding density of 5×10^2 cells/well. The cells were allowed to attach overnight, after which complete growth medium was replaced with starvation medium and the cells maintained in it as described in earlier. Subsequently the medium was replaced with starvation medium containing respective treatments as described earlier. Following initial treatments, the cells were incubated for 2 weeks at 37°C , in 5% CO_2 and 95% humidity with the careful change of treatment-containing medium every 96 hours. After 2 weeks, growth medium was taken off and the formed colonies were fixed with ice cold methanol (-20°C for 10 minutes) and subsequently, stained with 0.5%^{w/v} crystal violet solution. The crystal violet solution was then carefully rinsed off by submerging the wells in a container full of water until the dye stopped coming off. Afterwards, the colonies were allowed to dry at room temperature and images were obtained. Subsequently, the colonies were counted using ImageJ 1.46r software (NIH, USA) and percentage colony formation rates were calculated as described by Rice *et al.* ²⁵.

$$\% \text{ Colony formation rate} = \frac{n}{N} \times 100$$

Where n is the number of colonies counted, and is N is the seeding density

Selective cytotoxicity of CMERE in neoplastic prostate cells

The selective cytotoxicity of the hydroethanolic extract was determined using MTT assay. Briefly, human neoplastic 22Rv1 and BPH1 cells, and human THP1 monocyte-like cells were seeded into tissue culture-treated 96-well plates at a seeding density of 5×10^3 cells/well. The cells were allowed to attach overnight and normal growth medium was changed to treatment medium containing various concentrations of the hydroethanolic root extract (1, 3, 5, 10, 30, 50 and 100 mg/ml). The cells were treated for 72 hours. Absorbances were measured and IC_{50} s were determined as described in earlier. Subsequently, selective cytotoxicity of the extract was calculated as shown below ²⁶:

$$\text{Selectivity Index} = \frac{\text{IC}_{50} \text{ in normal cell}}{\text{IC}_{50} \text{ in neoplastic cell}}$$

Statistical analysis

Data are presented as Mean \pm SEM. The time-course curves were subjected to two-way repeated measures analysis of variance (ANOVA) with Tukey's multiple comparisons test. One-way ANOVA and students t tests were also used, depending on the type of data. Graphs were plotted using GraphPad Prism for Windows Version 8.01 (GraphPad, San Diego, CA, USA). Analysis of isobolograms were performed with the program Compusyn (version 1.0, Chou & Martin).

RESULTS and DISCUSSION

Previous chemical analysis of *C. membranaceus* revealed the presence of some compounds which have been shown to possess antiproliferative or cytotoxic activities against cancer cells. Crotomembranafuran, a furano-clerodane isolated from the plant has been shown to exhibit antiproliferative activity against human prostate cancer (PC-3) cells¹⁷. In addition, the plant has been shown to contain scopoletin and β -sitosterol which are known antiproliferative agents and may account in part for the antiproliferative effect of *C. membranaceus* extract against cancer cells¹⁷.

Gas chromatography mass spectrometry

In this study, GC-MS analysis revealed the presence of n-hexadecanoic acid which has been shown by previous studies to possess anticancer effects (Figure 1 and Table 1)²⁷. In addition to fatty acids, GC-MS analysis of the hydroethanolic extract also showed the presence of 9, 10-Secocholeasta, astaxanthin and prednisolone acetate, all of which have been shown by previous studies to possess anticancer activity²⁸.

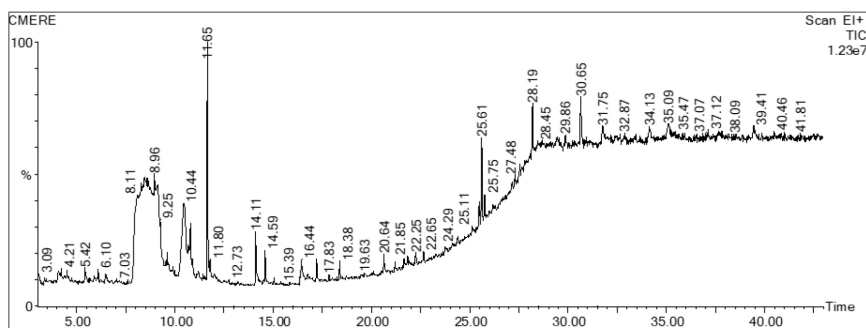


Figure 1. Gas chromatogram of *Croton membranaceus* hydroethanolic root extract

Table 1. GC-MS analysis for *Croton membranaceus* hydroethanolic root extract

#	RT	Area %	Norm %	Name
1	8.462	28.042	100.00	5-Hydroxypropanoic acid
2	8.957	11.588	41.32	Phenol, 3, 5-bis(1, 1-dimethylethyl)-
3	10.479	5.568	19.85	2-Octenoic acid, 5, 5, 7-trihydroxy
4	10.791	1.894	6.75	9, 10-Secocholesta-5,7,10(19)-triene-1,3-diol, 25-[(trimethylsilyloxy)-
5	11.653	3.274	11.67	Phenol, 4-(3-hydroxy-1-propenyl)-2-methoxy-
6	14.110	1.089	3.88	n-Hexadecanoic acid
7	25.606	1.331	4.75	Benzene, 1,2,4,5-tetrakis(1-methylethyl)-
8	30.648	1.387	4.95	Prednisolone acetate
9	31.748	1.147	4.09	1H, 4H-Pyrazolo[3,4-b]pyran-5-carbonitrile, 6-amino-4-(2, 4, 5-trimethoxyphenyl)-3-methyl-
10	35.085	1.130	4.03	Astaxanthin

GC-MS, gas chromatography mass spectrometry

CMERE is cytotoxic to human 22Rv1 prostate cancer cells

As GC-MS chromatograms showed the possible presence of cytotoxic compounds in the extract, it was hypothesized that the extract may inhibit the proliferation of human 22Rv1 CRPC cells. To investigate this effect, 22Rv1 cells were treated with different concentrations of either extract or the standard drug enzalutamide and cell proliferation was investigated using MTT assay. From the results obtained, enzalutamide was cytotoxic to 22Rv1 cells with an IC_{50} of 8.528 μ M (Figure 2A). Interestingly, the hydroethanolic extract also showed cytotoxic effect against the 22Rv1 cells with IC_{50} values of 3.809 mg/ml (Figure 2B). These findings indicate that enzalutamide and CMERE inhibit the proliferation of human 22Rv1 PCa cells. The inhibition of proliferation of 22Rv1 CRPC cells may be partly attributed to the anticancer principles shown to be present in CMERE by GC-MS analysis.

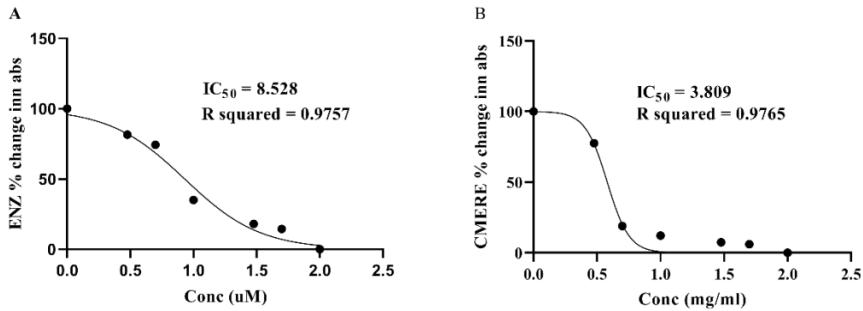


Figure 2. *Croton membranaceus* root extract is cytotoxic to human 22Rv1 prostate cancer cells. 22Rv1 cells were treated with varying concentrations of either enzalutamide or CMERE and cells were incubated for 72 hours. Cell viability was determined by MTT assay and absorbances were measured at 595 nm. All treatments were done in triplicates. (A) Enzalutamide-treated; (B) CMERE-treated.

CMERE inhibits testosterone-dependent and independent 22Rv1 cell proliferation

Having shown that *Croton membranaceus* root extract is cytotoxic to 22Rv1 cells, further investigations were conducted to determine if the inhibition was androgen-dependent or androgen-independent. Thus, the effects of the root extract were investigated in both testosterone-deprived and testosterone-supplemented environments. To investigate the effect of the extract on androgen-dependent cell proliferation, the growth medium was charcoal-stripped off steroid hormones to prevent interference with testosterone-dependent responses. Subsequently, the charcoal-stripped medium was supplemented with testosterone. Although supplementation of the growth medium with testosterone only resulted in a 0.3-fold increase in cell proliferation, the difference was still statistically significant when compared to the basal level cell proliferation (Figure 3).

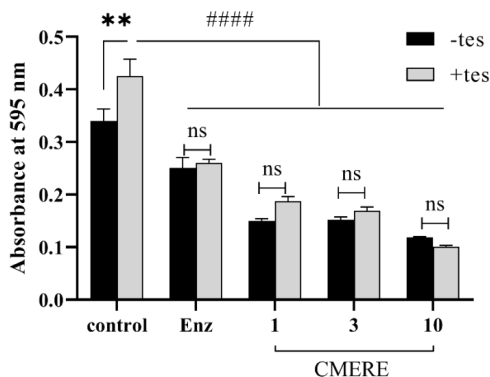


Figure 3. *Croton membranaceus* root extract inhibits testosterone-dependent and independent 22Rv1 cell proliferation. To investigate the effect of *C. membranaceus* extract on cell proliferation, 22Rv1 cells were treated over 72 hours with various concentrations of the hydroethanolic root extract. Cell proliferation was determined by MTT assay. Total inhibition of cell proliferation was calculated as AUC. Data is presented as mean \pm SEM. ** $p < 0.01$, hormone-independent control compared to hormone-treated control; #### $p < 0.0001$, extracts compared to hormone control; ns > 0.05 , extract in the absence of hormone compared to extract in the presence of hormone. Enz, enzalutamide.

Expectedly, treatment with the standard drug enzalutamide, significantly ($p < 0.01$) inhibited the proliferation of 22Rv1 cells compared to the untreated control (Figure 3) treatment with CMERE also significantly ($p < 0.0001$) inhibited testosterone-dependent proliferation of 22Rv1 cells compared to the solvent control (Figure 3). In addition, the extract significantly ($p < 0.001$) inhibited testosterone-independent proliferation of 22Rv1 cells, with less reductions in inhibitory effect compared to the inhibition of testosterone-dependent proliferation (Figure 3). However, there was no statistically significant difference between the effect of the extract on androgen-dependent and independent proliferation.

Combination of enzalutamide and CMERE synergistically inhibit 22Rv1 cell proliferation

It has been hypothesized that, drugs that act via similar mechanisms to achieve a common effect may likely produce additive effects when combined, whereas drugs that act through different mechanisms in achieving similar effects may interact synergistically²⁹. Both enzalutamide and CMERE have been shown, in this study, to achieve similar effects i.e., inhibition of 22Rv1 cell growth. In addition, combination of the two drugs inhibited 22Rv1 cell proliferation (Figure 4A). Thus, interaction between the two drugs was investigated using isobologram analysis. Isobologram analysis of the combination of CMERE and enzalutamide showed synergistic inhibition of 22Rv1 cell proliferation with CI values of

0.17, 0.26, 0.44, 0.70 and 0.99 for 50, 75, 90, 95 and 97% dose effect levels respectively (Figure 4B). From the results, r value of 0.977 obtained, indicated the conformity of the data to mass-action law. Most importantly, a normalized isobologram constructed at 90% fractional inhibition indicated synergy between the effect of enzalutamide and CMERE (Figure 4C). Thus, combination of the two drugs was synergistic in producing more than 90% cell kill effect in 22Rv1 cells, an effect very relevant in anticancer therapy. The results also showed favorable dose reduction index for the selected combinations, indicating a reduction in the probability of occurrence of an adverse effect when enzalutamide and CMERE are used as combination therapy (Figure 4D). In summary, results from isobologram analysis suggest the two drugs act via different mechanisms to achieve similar pharmacological effect. Thus, the effect of CMERE on 22Rv1 may largely be mediated via pathway(s) other than the androgen receptor-dependent pathways.

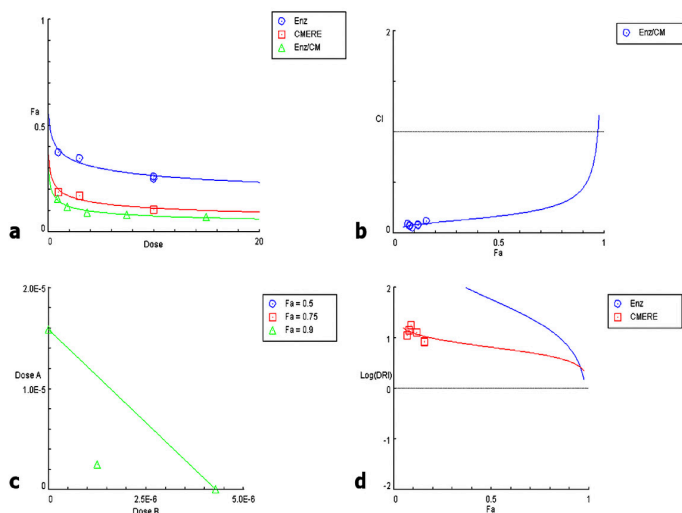


Figure 4. Combination of enzalutamide and CMERE synergistically inhibit 22Rv1 cell proliferation. MTT assay was used to obtain the dose effect curves. 22Rv1 cells were treated over 72 hours with various combinations of the EC50s of enzalutamide and CMERE. Additive effect (CI) = 1, synergism (CI < 1), and antagonism (CI > 1). (A) dose-effect curves; (B) combination index plot; (C) normalized isobologram at 90% dose-effect level; (D) Fractional inhibition-dose reduction index (DRI) plot.

Moreover, n-hexadecanoic acid shown by GC-MS analysis to be present in the hydroethanolic root extract is a known inducer of oxidative stress and apoptosis in cancer cells³⁰. In addition, the extract was shown by GC-MS to contain prednisolone acetate, which has been shown to inhibit androgen receptor-bypass mechanisms and also exert direct cytotoxic activity through the induction or suppression of specific cytokines. Thus, the extract may have inhibited 22Rv1

cell proliferation via restoration of apoptotic signals and modulation of glucocorticoid receptor-signaling which is an androgen-receptor bypass mechanism ³¹.

CMERE inhibits migration of human 22Rv1 prostate cancer cells

Cancer cell migration is a crucial step in the development of metastasis ³². Following the establishment of the antiproliferative effect of CMERE on 22Rv1 cells, the effect on collective cell migration was probed using the wound-healing assay. As shown in Figure 5, treatment with either enzalutamide or the extract reduced migration of 22Rv1 cells across the wounds created. Interestingly, treatment with all doses of the extract completely suppressed 22Rv1 cell migration within the first 24 hours of treatment (Figure 6A). Data from the different time points (Figure 6A) were used to calculate for total inhibition of cell migration by each treatment. From the results, CMERE significantly ($p < 0.0001$) inhibited the migration of 22Rv1 cells across the wound area (Figure 6B). Most notably, 10 mg/ml of the hydroethanolic suppressed migration of 22Rv1 cells across the wound area with cumulative percentage of $0.74 \pm 0.12\%$ compared to $84.19 \pm 1.79\%$ migration of the solvent control, representing $99.12 \pm 0.14\%$ suppression of cell migration (Figure 6B). This implies that the extract may inhibit migration of CRPC cells, which is a crucial step that precedes metastasis.

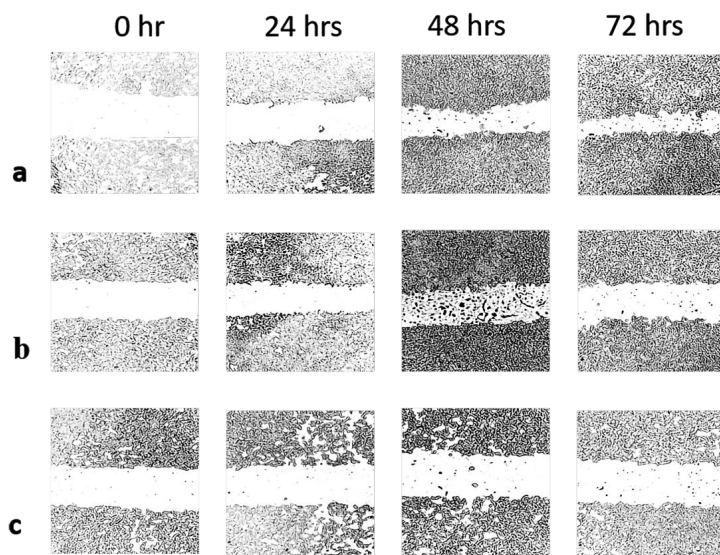


Figure 5. *Croton membranaceus* root extract inhibits human 22Rv1 cell migration. Human 22Rv1 cells were treated over 72 hours with various concentrations of either enzalutamide or CMERE. At confluence, monolayers were scratched with a 200 μ L pipette tip and photographed at 0, 24, 48 and 72 hours. (A) disease control; (B) enzalutamide-treated (10 μ M); (C) CMERE (10 mg/ml); CMERE, *Croton membranaceus* hydroethanolic root extract.

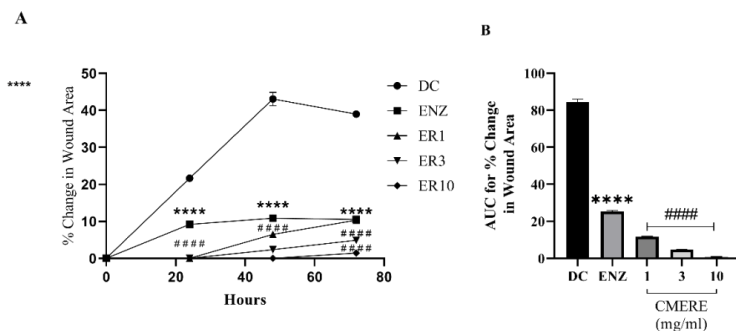


Figure 6. *Croton membranaceus* root extract suppresses overall migration of human 22Rv1 prostate cancer cells. To investigate the effect of *C. membranaceus* extracts on cell migration, 22Rv1 cells were treated over 72 hours with various concentrations of the hydroethanolic root extract. Cell motility was determined by wound healing assay. (A) CMERE time-course curve; (B) AUC for CMERE. Percentage wound closure was calculated as AUC. Data is presented as mean \pm SEM. *** $p < 0.001$, **** $p < 0.0001$. DC, disease control; ENZ, enzalutamide.

CMERE inhibit colony forming ability of human 22Rv1 prostate cancer cells

Furthermore, as shown in Figure 7, CMERE was identified in this study to inhibit the ability of human 22Rv1 PCa cells to form colonies. This implies that, the extract may inhibit the complex multiple stages of intra- and intercellular remodeling that cancer cells go through to stay alive and establish colonies^{30,33}. Metastasis remains a challenge to current treatment modalities and is the leading cause of cancer-related mortality³¹. Specifically, treatment with CMERE significantly ($p < 0.0001$) decreased the ability of 22Rv1 cells to form colonies with 10 mg/ml of the extract producing colony formation rate of $0.67 \pm 0.133\%$ compared to $43.00 \pm 1.31\%$ of the solvent control (Figure 8). This represents $98.44 \pm 0.31\%$ reduction in colony formation rate by the hydroethanolic extract, compared to the untreated control. In this regard, the inhibition of 22Rv1 colony formation by *C. membranaceus* root extracts suggests the ability of the extracts to inhibit the establishment of colonies post migration.

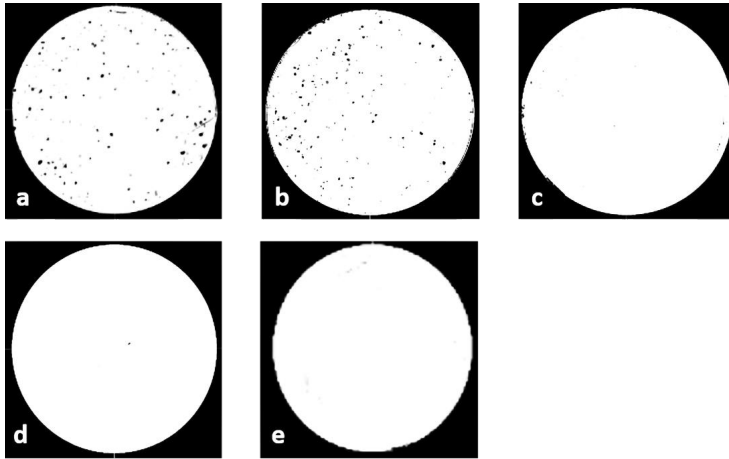


Figure 7. Colony-formation ability of human 22Rv1 prostate cancer cells is inhibited by CMERE. 22Rv1 cells (5×10^2 cells/well) were cultured for 14 days. Afterwards, colonies were fixed in ice cold methanol and stained with 0.5% w/v crystal violet solution. The wells were scanned and resulting images were analyzed with ImageJ software. (A) Disease control; (B) enzalutamide-treated (10 μ M); (C, D, E) CMERE (1, 3, 10 mg/ml).

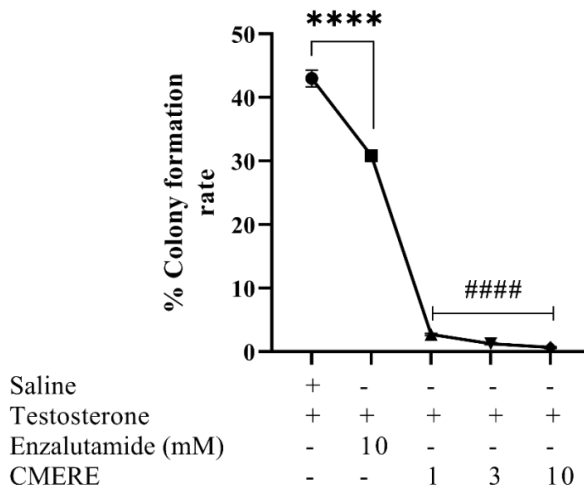


Figure 8. Colony-formation ability of human 22Rv1 prostate cancer cells is inhibited by *C. membranaceus* extract. 22Rv1 cells (5×10^2 cells/well) were cultured for 14 days. Afterwards, colonies were fixed in ice cold methanol and stained with 0.5% w/v crystal violet solution. Colonies were counted and graphed as percent colony formation over number of cells seeded. All treatments were done in triplicates. Total inhibition of colony formation was calculated as AUC. Data is presented as mean \pm SEM. **** $p < 0.0001$, enzalutamide compared to nontreated control; ##### $p < 0.0001$, extract compared to untreated control.

CMERE is selectively cytotoxic to human neoplastic prostate cells

Finally, to show that CMERE selectively inhibits human neoplastic 22Rv1 CRPC and BPH1 cells, but not normal human THP1 monocytes, comparative proliferation assay was carried out. As shown in Figure 9A and B, CMERE inhibited 22Rv1 and BPH1 cell proliferation with IC_{50} s of 3.809 mg/mL and 4.04 mg/mL, respectively. Conversely, CMERE did not inhibit the proliferation of THP 1 cells (Figure 9C). Suggesting that, the extract selectively inhibits the growth of neoplastic cells of prostate origin.

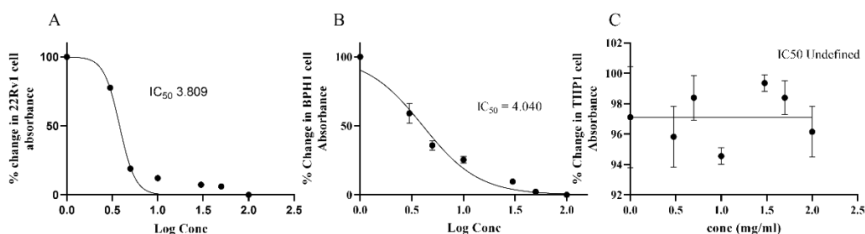


Figure 9. CMERE selectively inhibits human 22Rv1 prostate cancer and human BPH1 cells but not human THP1 monocyte-like cells. Human 22Rv1, BPH1 and THP1 cells were treated with varying concentrations of CMERE and subsequently cells incubated for 72 hours. Cell viability was determined by MTT assay. All treatments were done in triplicates. (A) 22Rv1; (B) BPH1; (C) THP1.

The lack of cytotoxic effect on human THP1 monocyte cells suggests that CMERE is selectively cytotoxic and treatment with it might not cause off-target effects. Accordingly, these findings support evidence from previous studies by Afriyie *et al.*³⁴ and Sarkodie *et al.*¹⁸ that reported safety of *C. membranaceus* hydroethanolic and aqueous extracts in rodent models. This differential cytotoxicity to human neoplastic cells makes *C. membranaceus* extracts particularly interesting as potential sources of safer drug leads in the management of CRPC.

In conclusion, this study has, for the first time, provided *in vitro* evidence that the hydroethanolic root extract of *Croton membranaceus* is effective in the inhibition of castration-resistant prostate cancer cell growth. Furthermore, combination of CMERE and enzalutamide synergistically inhibits more than 90% proliferation of 22Rv1 cells and holds the potential for the effective treatment of CRPC with less off-target effects. The findings from this study, however, cannot be directly extrapolated to humans. Further studies involving 3D cell cultures and xenograft models, which assess the role of the tumour microenvironment in cancer development and progression are therefore required to improve upon the acquired knowledge.

CONFLICT OF INTEREST

The authors declare that they have no known competing financial interests or personal relationships that could have appeared to influence the work reported in this paper.

AUTHOR CONTRIBUTIONS

KOY: Design, acquisition of data, analysis of data, drafting of manuscript, statistical analysis. ME: Design, acquisition of data. EAN: Design, critical review of manuscript, supervision. GHS: Design, Plant collection and authentication, GA: Design, critical review of manuscript, supervision.

ACKNOWLEDGEMENT

This work was supported by the KNUST College of Health Sciences Grant Award Scheme.

REFERENCES

1. Kang BJ, Jeun M, Jang GH, Song SH, Jeong IG, Kim CS, et al. Diagnosis of prostate cancer via nanotechnological approach. *Int J Nanomedicine*. 2015;10:6555-69. <https://doi.org/10.2147/IJN.S91908>.
2. Rawla P. Epidemiology of Prostate Cancer. *World J Oncol*. 2019;10(2):63-89. <https://doi.org/10.14740/wjon1191>.
3. Bray F, Ferlay J, Soerjomataram I, Siegel RL, Torre LA, Jemal A. Global cancer statistics 2018: GLOBOCAN estimates of incidence and mortality worldwide for 36 cancers in 185 countries. *CA Cancer J Clin*. 2018;68:394-424. <https://doi.org/10.3322/caac.21492>
4. Yeboah ED, Hsing AW, Mante S, Mensah JE, Kyei MY, Yarney J, et al. Management of prostate cancer in Accra, Ghana. *J West Afr Coll Surg*. 2016;6(4):31-65.
5. Dy GW, Gore JL, Forouzanfar MH, Naghavi M, Fitzmaurice C. Global burden of urologic cancers, 1990-2013. *Eur Urol*. 2017;71:437-446. <https://doi.org/10.1016/j.eururo.2016.10.008>
6. Ruizeveld de Winter JA, Janssen PJ, Sleddens HM, Verleun-Mooijman MC, Trapman J, Brinkmann AO, et al. Androgen receptor status in localized and locally progressive hormone refractory human prostate cancer. *Am J Pathol*. 1994;144(4):735-46.
7. Castanotto D, Zhang X, Ruger J, Alluin J, Sharma R, Pirrotte P, et al. A Multifunctional LNA Oligonucleotide-Based Strategy Blocks AR Expression and Transactivation Activity in PCa Cells. *Mol Ther Nucleic Acids*. 2020;23:63-75. <https://doi.org/10.1016/j.omtn.2020.10.032>.
8. Watson PA, Arora VK, Sawyers CL. Emerging mechanisms of resistance to androgen receptor inhibitors in prostate cancer. *Nat Rev Cancer*. 2015;15(12):701-711. <https://doi.org/10.1038/nrc4016>.
9. Wyatt AW, Gleave ME (2015). Targeting the adaptive molecular landscape of castration-resistant prostate cancer. *EMBO Mol Med*. 2015;7(7):878-894. <https://doi.org/10.15252/emmm.201303701>
10. Antonarakis ES, Lu C, Wang H, Lubner B, Nakazawa M, Roeser JC, et al. AR-V7 and resistance to enzalutamide and abiraterone in prostate cancer. *N Engl J Med*. 2014;371(11):1028-1038. <https://doi.org/10.1056/NEJMoa1315815>
11. Bastos DA, Antonarakis ES. Darolutamide For Castration-Resistant Prostate Cancer. *Onco Targets Ther*. 2019;12:8769-8777. <https://doi.org/10.2147/OTT.S197244>
12. Heidegger I, Brandt MP, Heck MM. Treatment of non-metastatic castration resistant prostate cancer in 2020: What is the best? *Urol Oncol*. 2020;38(4):129-136. <https://doi.org/10.1016/j.urolonc.2019.11.007>
13. Maroyi A. Review of *Croton membranaceus* Mull. Arg.: phytochemical, pharmacological and toxicological perspective. *J Complement Med Res*. 2018;9(1):24-33. <https://doi.org/10.5455/jcmr.20180718123349>
14. Dutta S, Mahalanobish S, Saha S, Ghosh S, Sil PC. Natural products: An upcoming therapeutic approach to cancer. *Food Chem Toxicol*. 2019;128:240-255. <https://doi.org/10.1016/j.fct.2019.04.012>
15. Amani SA, Reham ME, Gamal AS. Natural products in the treatment of ulcerative colitis and peptic ulcer. *J Saudi Chem Soc*. 2013;17(1):101-124. <https://doi.org/10.1016/j.jscs.2012.03.002>
16. Asare GA, Adjei S, Afriyie D, Appiah-Danquah AB, Asia J, Asiedu B. Genotoxic and cytotoxic activity of aqueous extracts of *Croton membranaceus* in rodent bone marrow and

human benign prostate hyperplasic cells. *European J Med Plants*. 2015;9(2):1–7. <https://doi.org/10.9734/EJMP/2015/18583>

17. Bayor MT, Ayim JS, Marston G, Phillips RM, Shnyder SD, Wheelhouse RT, et al. A cytotoxic diterpenoid from *Croton membranaceus*, the major constituent of anticancer herbal formulations used in Ghana. *Nat Prod Commun*. 2008;3(11):1875-1878. <https://doi.org/10.1177/1934578X080030111>

18. Sarkodie JA, Appiah AA, Edoh DA, Aboagye FA, Asiedu-Larbi J, Tandoh M, et al. Antihyperglycaemic and antioxidant effects of *Croton membranaceus* Mull. Arg (Euphorbiaceae). *Int J Pharm Sci Res*. 2014;5(1):110–5. [https://dx.doi.org/10.13040/IJPSR.0975-8232.5\(1\).110-15](https://dx.doi.org/10.13040/IJPSR.0975-8232.5(1).110-15)

19. Ullah R, Bakht J, Shah MR. GC-MS analysis of bioactive compounds present in medicinally important *Periploca hydaspidis*. *Pak J Pharm Sci*. 2019;32(4):1615–1619.

20. Khurana N, Kim H, Chandra PK, Talwar S, Sharma P, Abdel-Mageed AB, et al. Multimodal actions of the phytochemical sulforaphane suppress both AR and AR-V7 in 22Rv1 cells: Advocating a potent pharmaceutical combination against castration-resistant prostate cancer. *Oncol Rep*. 2017;38:2774-2786. <https://doi.org/10.3892/or.2017.5932>

21. Zhao Y, Cheng X, Wang G, Liao Y, Qing, C. Linalool inhibits 22Rv1 prostate cancer cell proliferation and induces apoptosis. *Oncol Lett*. 2020;20(6):289. <https://doi.org/10.3892/ol.2020.12152>

22. Song W, Khera M. Physiological normal levels of androgen inhibit proliferation of prostate cancer cells in vitro. *Asian J Androl*. 2014;16(6):864–868. <https://doi.org/10.4103/1008-682X.129132>

23. Chou TC. Drug Combination Studies and Their Synergy Quantification Using the Chou-Talalay Method. *Cancer Res*. 2010;70(2):440–6. <https://doi.org/10.1158/0008-5472.CAN-09-1947>

24. Chou TC, Talalay P. Analysis of combined drug effects: a new look at a very old problem. *Trends Pharmacol Sci*. 1983;4:450–4. [https://doi.org/10.1016/0165-6147\(83\)90490-X](https://doi.org/10.1016/0165-6147(83)90490-X)

25. López-Lázaro M. How many times should we screen a chemical library to discover an anticancer drug? *Drug Discov Today*. 2015;20:167–169. <https://doi.org/10.1016/j.drudis.2014.12.006>

26. Rice MA, Hsu EC, Aslan M, Ghoochani A, Su A, Stoyanova T. Loss of Notch1 Activity Inhibits Prostate Cancer Growth and Metastasis and Sensitizes Prostate Cancer Cells to Antiandrogen Therapies. *Mol Cancer Ther*. 2019;18(7):1230-1242. <https://doi.org/10.1158/1535-7163.MCT-18-0804>

27. Yoo YC, Shin BH, Hong JH, Lee J, Chee HY, Song KS, et al. Isolation of fatty acids with anticancer activity from *Protaetia brevitarsis* larva. *Arch Pharm Res*. 2007;30(3):361-5. <https://doi.org/10.1007/BF02977619>

28. McCall B, McPartland K, Moore R, Frank-Kamenetski A, Booth BW. Effects of astaxanthin on the proliferation and migration of breast cancer cells in vitro. *Antioxidants*. 2018;7(10):135. <https://doi.org/10.3390/antiox7100135>

29. Matsumura N, Nakaki T. Isobolographic analysis of the mechanisms of action of anti-convulsants from a combination effect. *Eur J Pharmacol*. 2014;741:237-246. <https://doi.org/10.1016/j.ejphar.2014.08.001>

30. Massagué J, Obenauf AC. Metastatic colonization by circulating tumour cells. *Nature*. 2016;529(7586):298-306. <https://doi.org/10.1038/nature17038>

31. Montgomery B, Cheng HH, Drechsler J, Mostaghel EA. Glucocorticoids and prostate cancer

treatment: friend or foe? *Asian J Androl.* 2014;16(3):354-8. <https://doi.org/10.4103/1008-682X.125392>

32. Yamaguchi H, Wyckoff J, Condeelis J. Cell migration in tumors. *Curr Opin Cell Biol.* 2005;17(5):559-564. <https://doi.org/10.1016/j.ceb.2005.08.002>

33. Klusa D, Lohaus F, Furesi G, Rauner M, Benešová M, Krause M, et al. Metastatic Spread in Prostate Cancer Patients Influencing Radiotherapy Response. *Front Oncol.* 2021;10:627379. <https://doi.org/10.3389/fonc.2020.627379>

34. Afriyie DK, Asare GA, Bugyei K, Asiedu-Gyekye I, Gyan BA, Adjei S, et al. Anti-atherogenic and anti-ischemic potentials of *Croton membranaceus* observed during sub-chronic toxicity studies. *Pharmacognosy Res.* 2013;5(1):10-6. <https://doi.org/10.4103/0974-8490.105640>